# The effects of beam-column connections
# on behavior of buckling-restrained braced frames

Mohammad Ali Hadianfard [*1], Fateme Eskandari [1a] and Behtash JavidSharifi [2b]

[1] *Department of Civil and Environmental Engineering, Shiraz University of Technology, Shiraz, Iran*
[2] *Fars Regional Electric Company*

**Abstract.** Buckling Restrained Braced (BRB) frames have been widely used as an efficient seismic load resisting system in recent years mostly due to their symmetric and stable hysteretic behavior and significant energy dissipation capacity. In this study, to provide a better understanding of the behavior of BRB frames with various beam-column connections, a numerical study using non-linear finite element (FE) analysis is conducted. All models are implemented in the Abaqus software package following an explicit formulation. Initially, the results of the FE model are verified with experimental data. Then, diverse beam-column connections are modeled for the sake of comparison from the shear capacity, energy dissipation and frame hysteresis behavior points of view until appropriate performance is assessed. The considered connections are divided into three different categories: (1) simple beam-column connections including connection by web angle and connection by seat angle; (2) semi-rigid connection including connection by web and seat angles; and (3) rigid beam-column connections by upper-lower beam plates and beam connections with web and flange splices. Results of the non-linear FE analyses show that these types of beam-column connections have little effect on the maximum story drift and shear capacity of BRB frames. However, the connection type has a significant effect on the amount of energy dissipation and hysteresis behavior of BRB frames. Also, changes in length and thickness of the angles in simple and semi-rigid connections and changes in length and thickness of plates in rigid connections have slight effects (less than 4%) on the overall frame behavior.

**Keywords:** Buckling Restrained Brace (BRB); rigid connection; simple connection; braced frame; energy dissipation

## 1. Introduction

In comparison with other lateral seismic systems, Buckling Restrained Braced (BRB) frames dissipate more amounts of hysteretic energy during earthquake. Since BRBs yield in compression as they do in tension, they show properly stable cyclic behaviors and this performance develops the energy dissipation capacity and ductility significantly. In such frames, a steel core that carries the entire axial load is placed inside a steel tube that restrains the core against buckling. The steel tube is filled by grout and encompasses a thin coating or gap placed around the core plate to prevent shear stress transfer to the grout or the steel tube.

BRB has been applied in several building structures as an economic seismic load resisting system. This property of BRB systems was proven by Tremblay *et al.* (2004). The performance of BRB has been explored by numerous experimental and numerical analyses, Watanabe *et al.* (1998) implemented component tests to indicate the effect of the outer tube configuration on system performance.

Clark *et al.* (1999) compared the performance of BRB frames and moment-resisting frames from the point of view of story drift and base shear. They showed that the performance of BRB frames is better than that of moment-resisting frames.

The behavior of gusset plates and bracing connections has been studied by numerous researchers including Hadianfard *et al.* (2015), Hadianfard and Khakzad (2016) and Hadianfard *et al.* (2017). These researchers have studied the non-linear and post-buckling behaviors of gusset plates and effects of various bracing connections on seismic behavior of braced frames. However, not enough attention has yet been paid to the role of beam-column connections on the behavior of braced frames. Aiken *et al.* (2002) conducted experimental cyclic tests on BRB frames with welded beam-column connections and continuous beams. This is referred to as moment connections and bolted brace-gusset connections and is shown in Fig. 1(a). Fahnestock *et al.* (2007) tested a four story BRB frame with chevron braces designed based on AISC (2005) and ASCE (2005) considerations for a site with stiff soil in Los Angeles, California. In their experimental research, pinned brace-gusset and bolted splice beam-to-beam connections, as shown in Fig. 1(b), were used. Christopulos (2005) tested five BRB frames with bolted brace-gusset connections and investigated the effects of different geometries of gusset plates on failure modes. Prinz (2007) used a non-linear dynamic analysis to inspect the effects of beam splices on

*Corresponding author, Ph.D., Associate Professor,
  E-mail: hadianfard@sutech.ac.ir
[a] M.Sc. Student, E-mail: fatemeeskandari991@gmail.com
[b] Superintendent of Construction Projects,
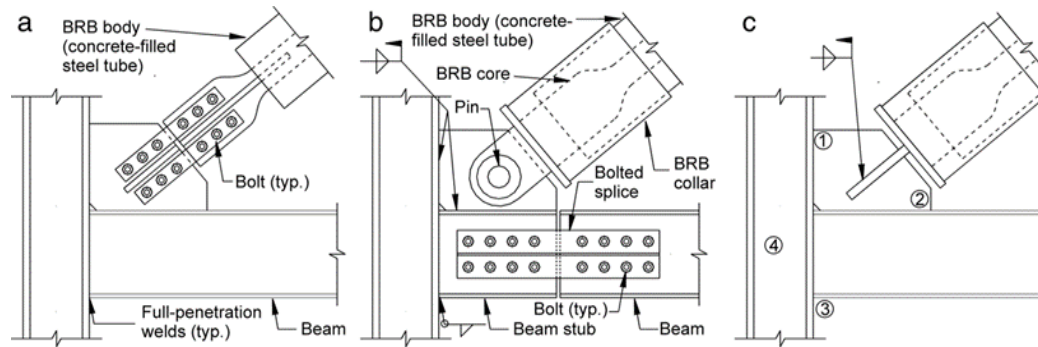  E-mail: b.javidsharifi@sutech.ac.ir

Fig. 1 BRB connection details: (a) continuous beam, bolted brace; (b) spliced beam, pinned brace; (c) continuous beam, welded brace (Wigle and Fahnestock 2010)

the BRB frame behavior. The research results showed that the impact of beam splices on the BRB frame performance cannot be negligible. Wigle and Fahnestock (2010) used a finite element model to investigate the third story of the four-story BRB frame previously tested by Fahnestock *et al.* (2007). The researchers prepared a three dimensional FE model and verified it with experimental data. They used the non-linear FE models to study the behavior of beam-column-brace connections as shown in Figs. 1(b) and (c). The results showed that the influence of beam-column-brace connection configurations on the behavior and performance of BRB frames are not negligible. Chou *et al.* (2014) developed a new steel dual-core self-centering brace (DC-SCB) and evaluated its cyclic performance. Also, Chou and Chung (2014) proposed an innovative steel dual-core self-centering brace (SCB) that provides the structure not only with energy dissipation but also with re-centering properties. This reduces the residual drift of the braced structure during earthquakes.

To consider other aspects of the subject, size and type effects of the filler material in the gap at the steel core-concrete interface were investigated by Talebi *et al.* (2015) where the BRBs' fire resistance capacity was inspected. The study showed that the highest efficiency in resistance against fire by the BRB was obtained by replacing the metal filler material in the gap with concrete as well as by increasing the dimensions of the gap. Fanaie and Afsar Dizaj (2014) calculated the over-strength, ductility and response modification factors for BRB frames with reduced length (RL) that is considered in one end of the brace element. Results showed that the mentioned parameters of this type of BRB frames are greater than those in the conventional types. Furthermore, better seismic performance was observed in RLBRB frames. Apart from that study, RLBRB was also studied by Razavi-Tabatabaei *et al.* (2014). The major results of the research showed that RLBRB exhibits large energy dissipation capacity compared to the conventional full-length BRB. Finally, both recently mentioned researches show that RLBRBs have desirable performance, especially when placed at the end part of the brace. In that respect, an experimental research was also conducted by Palmer *et al.* (2014). The performance of a large-scale BRB frame system with gusset plate connections was evaluated. How influential connection configuration is on the seismic behavior of BRB

frames rather than isolated BRBs was addressed. It was reported that the hysteretic performance of BRB frames is very appropriate for moderate inelastic deformations; sever damages may occur at large story drifts and possible unexpected fracture of beam-column connections may lead to undesirable behavior.

Additional experimental research has been executed by Lin *et al.* (2012), wherein a series of hybrid and cyclic loading tests were conducted on a three-story single-bay full-scale BRB frame. Also, Kim and Choi (2015) carried out monotonic loading tests, cyclic loading tests and finite element analyses on inverted V-braced frames reinforced with non-welded buckling-restrained braces. Furthermore, supplementary numerical and finite element researches on BRB frames have been performed by Ghowsi and Sahoo (2015), Assaleh *et al.* (2015) and Flogeras and Papagiannopoulos (2017).

Several recent large scale experimental and numerical studies have shown that while BRB frames display appropriate performance, due to the undesirable failure mode of the connection, some limitations do exist. In other words, the behavior of the connections of a BRB frame is very important and can affect the seismic behavior of the frame. Therefore, this study aims to focus on the beam-column connections of BRB frames to extend the results from previous researches.

In this research, in order to reach an optimum seismic design at which most of the energy dissipating potential and ductility is utilized, different beam-column connections including simple, semi-rigid and rigid connections are modeled. Classification of steel connections into three groups of simple, semi-rigid and rigid connections is a common technique seen in many specifications such as ANSI/AISC 360-10 (2010) and Eurocode 3-Part 1-8 (2005), and has been the subject of numerous researches such as Hadianfard and Rahnema (2010) and Faridmehr *et al.* (2016). The fundamental criteria considered in categorization of the connections is the moment-rotation (M-θ) curve of the connection, where strength, stiffness and ductility of the connections are the main classification parameters. However, some differences exist among these specifications in terms of connection classification schemes. On the other hand, the boundaries between the different classes are not completely clear and are not the same in all specifications.

In the present study, hysteretic behaviors of various frames with different connections are obtained and the achieved energy dissipation potentials and maximum story drifts are compared for different connections, and finally the most appropriate beam-column connection is characterized. Therefore, this paper intends to extend the experimental researches of Palmer *et al*. (2014) through finite element modeling of single-story plane frames which have already been tested by Palmer *et al*. (2014). At first, the finite element model is verified by the experimental results of Palmer *et al*. (2014). Then, various beam-column connections are considered to explore the effects of different beam-column connection configurations on the hysteretic performance and accordingly ductility and energy dissipation capacity of BRB frames.

## 2. Modeling process

### 2.1 Experimental model

The prototype frames tested by Palmer *et al*. (2014) consisted of six large-scale single-story and one-bay planar BRB frames as shown in Fig. 2. The frames were chosen to
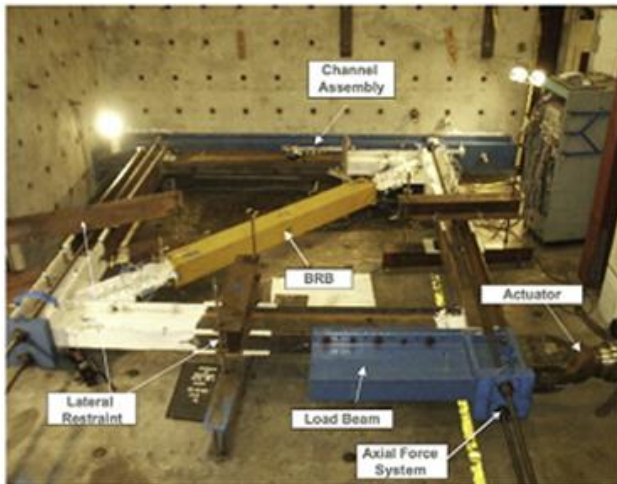


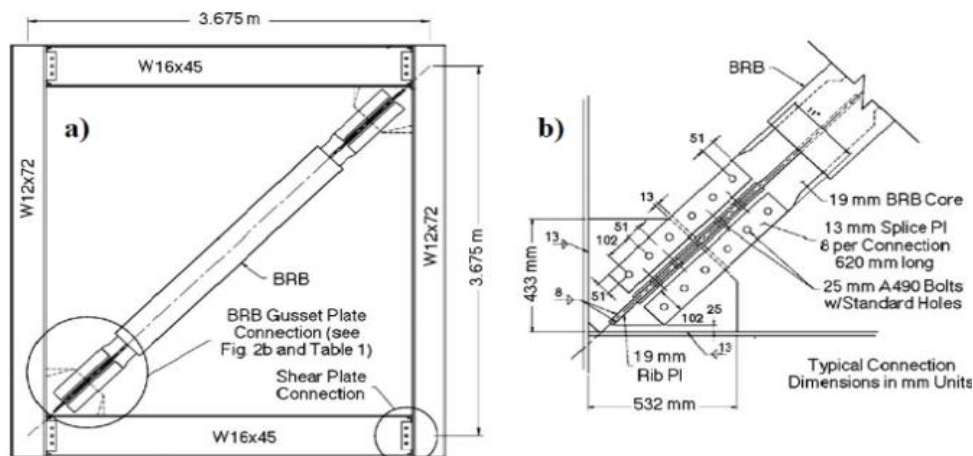Fig. 2 Test setup of BRB frame (Palmer *et al*. 2014)

explore the effects of different gusset configurations. The geometry and component sizes were as illustrated in Fig. 3(a). Column spacing and story heights were all equal to 3.68 m. The reference gusset plates had a thickness of 19 mm and were connected to the beams and columns. To study the details of the connections, the tests were focused on BRBs with bolted connections as shown in Fig. 3(b).

The typical BRB frame had wide flange beams and columns, sized W16×45 and W12×72, respectively, made of ASTM A992 steel. The experienced structures produced input data for designing BRB frames according to AISC (2005). The length of the BRB was 3.6 m, and it was made from a 19×162 mm rectangular core plate with a length of 2.34 m and a 250×250×6 mm steel tube restrainer casing with infill grout.

### 2.2 The finite element model

The general shape of the BRB frame modelled in the Abaqus v6.12 (2012) software is depicted in Fig. 4(a). The reference gusset plates were connected to the beams and columns according to Fig. 3(b) and as illustrated in Fig. 4(b).

The selection and calibration of material properties and hardening parameters were based on the cyclic test results conducted by Palmer *et al*. (2014), as given in Table 1. For

Table 1 Material plastic properties

| Frame members | Stress (N/mm$^2$) | $F_y$ | $F_y$ | $F_u$ | $F_u$ |
|---|---|---|---|---|---|
| | Residual strain | 0 | 3$\epsilon_y$-$F_y$/E | $\epsilon_u$-$F_u$/E | 1.1$\epsilon_u$-$F_u$/E |
| Core | Stress (N/mm$^2$) | 240 | 240 | 370 | 370 |
| | Residual strain | 0 | 0.0024 | 0.023417 | 0.025943 |
| Beam | Stress (N/mm$^2$) | 379 | 379 | 507 | 507 |
| | Residual strain | 0 | 0.00379 | 0.024483 | 0.027185 |
| Column | Stress (N/mm$^2$) | 407 | 407 | 468 | 468 |
| | Residual strain | 0 | 0.00407 | 0.013932 | 0.015559 |
| Gusset plate | Stress (N/mm$^2$) | 345 | 345 | 450 | 450 |
| | Residual strain | 0 | 0.00345 | 0.020425 | 0.022693 |



Fig. 3 Plane BRB frame experiments: (a) frame geometry; (b) typical BRB connection (Palmer *et al*. 2014)
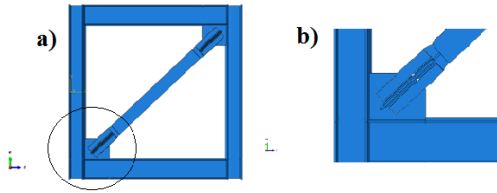
Fig. 4 Finite element model: (a) frame geometry;
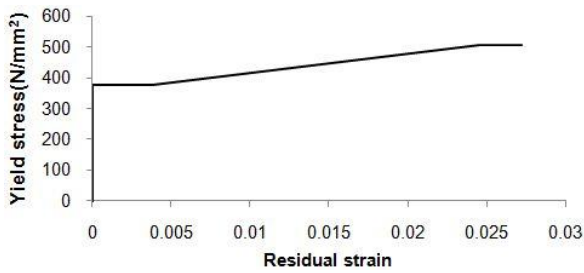(b) typical BRB connection



Fig. 5 Yield stress-plastic strain curve of beam material

example, the yield stress-plastic strain curve relevant to the material of the beam, as shown in Fig. 5, was applied to the Abaqus model. The elastic modulus and Poisson's ratio of all steel components were respectively 200 GPa and 0.3. Young modulus of 23 GPa and Poisson's ratio of 0.2 were assumed for the infill grout.

The steel material model was assumed to follow the Von Mises yielding criterion. For the core steel, mixed plasticity including kinematic and isotropic hardening was used. To reproduce the inelastic material property of other members a plasticity isotropic hardening rule was employed. The change of backstress is presented by the kinematic component according to the plastic strain. The change in the size of the yield surface, on the other hand, is defined by the isotropic component as a function of the equivalent plastic strain (Razavi-Tabatabaei *et al*. 2014). To simulate material plastic properties, yield stress was applied to the Abaqus model according to the remained plastic strain relevant to the frame members, as discussed in the following.

The linear portion of the curve is the elastic region whose slope equals Young's modulus. Prior to the yield point, the material will deform elastically and will return to its original shape when the applied stress is removed. Then, the residual strain will be zero. Past the elastic limit, the yield stress is constant until the strain limit is reached ($3\varepsilon y$). In this step, the unloading curve is parallel to the initial elastic loading curve. After unloading, there is a certain amount of elastic recovery ($Fy/E$) and some residual strain ($3\varepsilon y - Fy/E$). The maximum stress in this diagram is the ultimate stress ($Fu$) and the corresponding strain is ($\varepsilon u$). The residual strain will equal ($\varepsilon u - Fu/E$). In the Abaqus model the ultimate stress does not change until the residual strain reaches ($1.1\varepsilon u - Fu/E$).

The FE model included the core plate, the encasing member, end stiffeners, gusset plates and other plates for modelling various different simple, semi-rigid and rigid connections. Since solid elements would suitably capture the localized stress and strain demands within the

connections, all steel members were modeled using solid elements. A relatively fine mesh with element size of 50 mm was used for simulation of the member parts. By changing the mesh size (40, 50 and 60 mm), the accuracy of modeling and mesh dependency were checked. The final mesh size (50 mm) had enough accuracy.

Because the core element would undergo large plastic deformations and large higher mode buckling, it was modelled using C3D20 quadratic brick elements. This element is proper for large displacements and therein each of the 20 nodes has 3 translational degrees of freedom (Abaqus v6.12 Users' Manual 2012). So, the core plate was modelled using a 20-node C3D20 element and the other elastic components were modelled using 8-node C3D8 brick elements with reduced integration. Selection of C3D20 for the core element and C3D8 for other parts can result in reduction of the computational cost (Razavi-Tabatabaei *et al*. 2014). A large-displacement cyclic analysis was performed using Abaqus (2012). The full Newton-Raphson method was considered for solving the non-linear equations of the analysis (Hoveidae and Rafezy 2012). The connections details were modelled according to Palmer *et al*. (2014). Since no slipping existed between the core plate and the restraining member, rigid beams were used to simulate all bolted connections. The side plates shall have proper holes to account for the bolts passing through the rigid beams. In this paper, instead of modelling the bolts or the holes, the corresponding nodes in the connected parts were slaved to represent force transfer through bolt bearing. In addition, full attachment was provided at all welded interfaces using either tie constraints or shared nodes, according to Wigle and Fahnestock (2010). The steel core was modelled to be interactive with a restraining member with a hard contact behavior, allowing the separation of the interface in tension and letting no penetration in compression (Chou and Chen 2010). A frictional coefficient of 0.1 was adopted to simulate the greasy grout-restraining member interface. Constraint equations were defined to constrain the movement of the encasing to the centre of the core (Razavi-Tabatabaei *et al*. 2014). The loading protocol prescribed by the AISC (2005) was used. To model the imported load, a set of displacements according to Fig. 6 were applied to two reference points located on the lower beam as shown in Fig. 7. The peak displacements of the test were imposed to the two ends of the lower beam in the
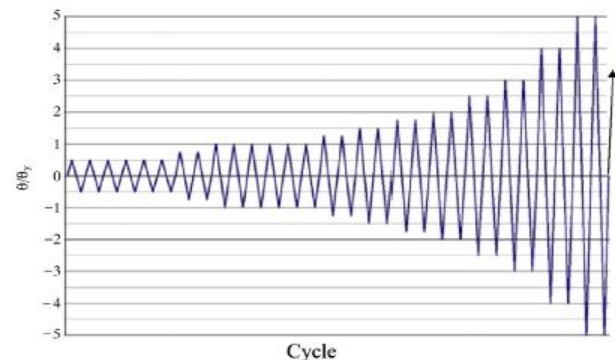


Fig. 6 Plane frame deformation history (Hadianfard *et al*.
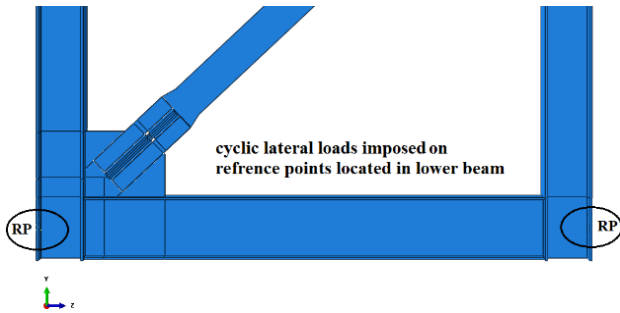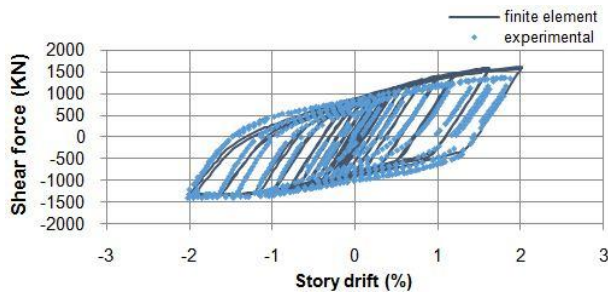2017)

Fig. 7 Imposition of cyclic lateral loads



Fig. 8 Reaction force-story drift verification

form of axial displacements, while the other beam was assigned to be in a fixed condition in all of its degrees of freedom. The axial force was derived from the force resultants on the fixed end plate of the upper beam (Razavi-Tabatabaei *et al*. 2014).

### 2.3 Verification

To verify the precision of the conducted FE model, the displacements were applied to the FE model. The out-of-plane deformations were confined by imposing initial boundary conditions on the beams and columns. The reaction force-story drift curve is captured from the outputs of the FE analysis and shown in Fig. 8. These results are compared with the experimental results. The hysteresis curve is suggestive of strength deterioration caused by global or local buckling or formation of plastic hinges. Also, numerical values of maximum shear capacities and the corresponding story drifts of the frame are compared in Table 2. The comparison between the FE analysis outputs and the experimental results shows appropriate accordance between the numerical simulation and the experiment. The FE model was accepted to be adequate for parametric studies because its purpose has been to make relative comparisons between beam-column connection configurations without any change in the BRB core geometry and yield region, and hence the limitations of the model related

Table 2 Numerical comparison between the finite element analysis and experimental results

| Parameters | Experiment | FE model | Error (%) |
| --- | --- | --- | --- |
| Shear capacity (KN) | 1468.72 | 1619.85 | 9.33 % |
| Story drift (%) | 1.88 | 2.02 | 6.9 % |

to the confinement effects on BRB core were considered to be non-critical (Wigle and Fahnestock 2010).

### 2.4 Behavior assessment

In the field of steel core behavior during the steps of the analysis, Razavi-Tabatabaei *et al*. (2014) expressed that in early cycles of loading buckling of the core occurs about the weak axis which comes into contact with the encasing at both ends. However, when the axial demand increases, the core buckles about the strong axis forming a sinusoidal shape. Soon after buckling, the edges of the core find supports close and stiff enough to let the member keep up with load bearing capacity. Later in higher compressive forces, as soon as the core yields the core plate buckles in higher modes in the out-of-plane direction. The local buckling puts the core and the encasing into contact which results in higher load carrying capability (Razavi-Tabatabaei *et al*. 2014). Herein, to reduce the computational cost, a simplified behavior for the core simulation is used. This purpose was achieved by elimination of core encasing from the FE model and followed by restricting the out-of-plane movement of the core plate to prevent the core from buckling about the weak axis by imposing initial boundary conditions on the core element. Other initial boundary conditions were imposed on 3 points located on the core plate to prohibit the core from buckling about the strong axis. The reference model explained above was used to later consider the behavior of various beam-column connection configurations. Thus, the different cases include simple and semi-rigid beam-column connections by angles and rigid beam-column connections by direct welding, upper-lower beam plates and beam web and flange splice connections all studied to obtain influences of the variations on the frame behavior. Since the bolts were assumed to be slip-critical, the welded connections were chosen to connect the plates to the beams and columns. Like other welded interfaces in the model, these welded interfaces were modelled as fully attached using tie constraints.

In all FE models, the sections of the beams and columns were constant and were selected as the experimental model of Palmer *et al*. (2014) which was previously used for verification of the finite element model. Primary design of the connections was done based on the dimensions of the beams and columns and their bending and shear capacities.

## 3. Finite element parametric studies

### 3.1 Description of the finite element models

Each frame model was loaded under a displacement pattern identical to Fig. 6 which was similar to the experimental cyclic load. The out-of-plane deformations were prevented via imposing initial boundary conditions on the frame elements. The results are focused on in-plane responses. In this study the frame shear capacity corresponding to the applied displacements with emphasis on beam-column connection configurations is obtained. The simple beam-column connections contain web angle connections and seat angle connections. The semi-rigid
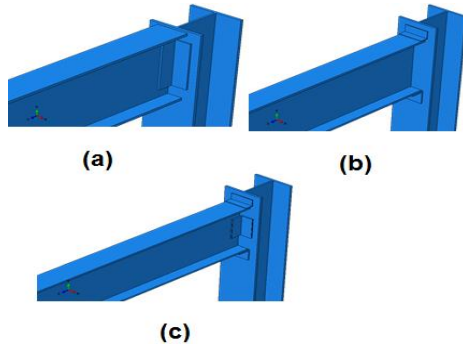
Fig. 9 Modeled simple and semi-rigid connections:
(a) simple connection by web angle; (b) simple
connection by seat angle; (c) semi-rigid
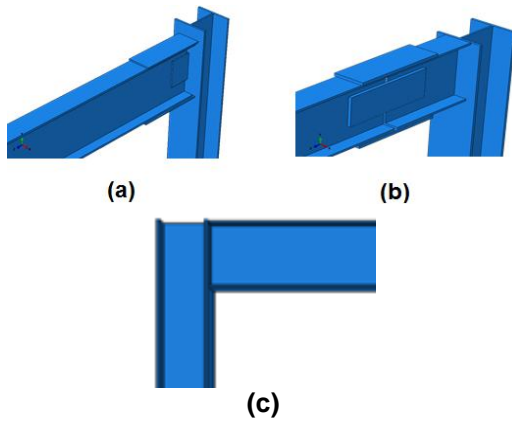connection by web and seat angles



Fig. 10 Modeled rigid connections: (a) connection
with upper-lower beam plates; (b) connection
with beam web and flange splices; (c) direct
welded rigid connection

connection contains combined web and seat angle connections. The modeled simple and semi-rigid connections in Abaqus are illustrated in Fig. 9. Also, the configuration of the rigid beam-column connection by direct welding, upper-lower beam plates and the beam connection with web and flange splices are depicted in Fig. 10.

### 3.2 Results of the finite element analysis

For all BRB frames with various beam-column connections, shear bearing capacities, maximum story drifts and energy dissipations are calculated. Connection tags are given in Table 3.

Table 3 Connection numbers

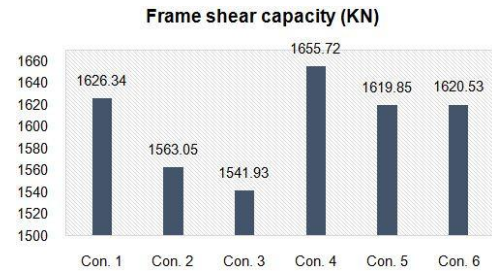| Simple & semi-rigid connections | | | Rigid connections | | |
|---|---|---|---|---|---|
| Con.1 | Con.2 | Con.3 | Con.4 | Con.5 | Con.6 |
| Web and seat angles | Seat angle | Web angle | Upper-lower beam plates | Welded con. | Beam web and flange splices |



Fig. 11 Shear capacity of frames with different connections

The shear bearing capacity of each connection configuration is presented in Fig. 11. This figure shows minor difference in the frame shear bearing capacity for different connections. For example, a comparison of shear capacity values between the frames with rigid connections with upper-lower beam plates (Con.4) and those with simple connections by web angles (Con.3) reveals a difference of 8%. This comparison shows that the difference of shear capacities between a frame with rigid and one with simple connections is less than 10%. In other words, in BRB frames the braces control the lateral behavior, and beam-column connections do not play a major role. A comparison between the shear capacity of the frame with rigid connections and continuous beams (welded rigid connection, Con.5) and one involving rigid connections with beam splices (Con.6) shows that the shear capacities are almost equal and have only a slight difference (about 2%) with a frame that has rigid connections with upper-lower beam plates (Con.4).

Furthermore, the comparison between the shear capacities of frames with simple and semi-rigid connections shows that by increasing the rigidity of the connections, the frame's shear capacity slightly increases. For example, the difference between a simple connection with a web angle (Con.3) and a semi-rigid connection with web and seat angles (Con.1) is roughly about 5%.

For the different connection cases there was little variation in the maximum story drift and all cases reached the story drift angle of approximately 2%. So, no comparison of these quantities is presented.

The amount of energy dissipated in the structure under cyclic loading equals the area inside the hysteresis curve. The dissipated energy increases as the imposed displacement and the contact forces increase (Hoveidae and Rafezy 2012). Energy dissipation of the frames are compared in Fig. 12. The results show that the type of beam-column connection has a significant impact on the dissipated energy. The rigid connection with beam web and flange splices (Con.6) and the one with upper-lower beam plates (Con.4) had better energy dissipation capability compared to the other connections. For instance, the energy dissipation capability of the frame with rigid connections of type Con.6 was 25% greater compared to the frame with rigid connections of type Con.5. Furthermore, the difference between Con.6 (rigid) and Con.3 (simple) was about 17%. This considerable difference is due to different behaviors of the connections under cyclic loading. The hysteresis curves of Con.5 and Con.6 are compared in Fig. 13. This figure shows that the area inside the hysteresis curve of Con.6 is
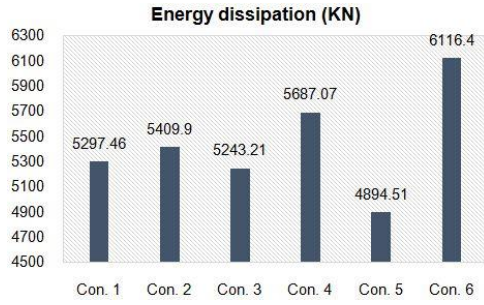
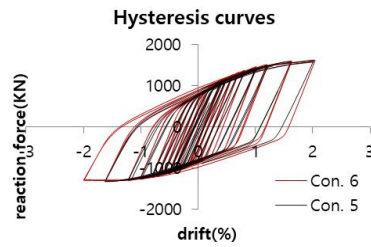Fig. 12 Energy dissipation of different connection configurations



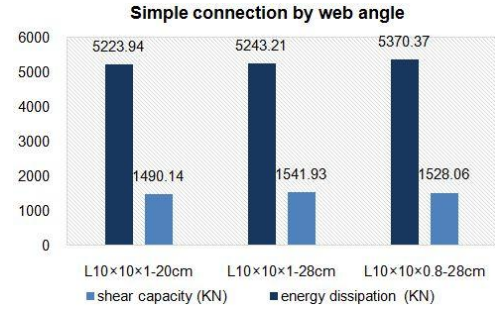Fig. 13 Comparison of hysteresis curves of Con.5 and Con.6.



Fig. 14 Simple connection with web angles of various lengths and thicknesses
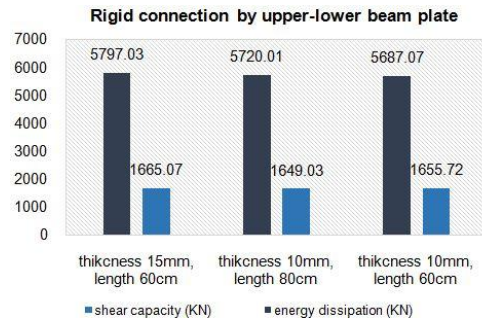


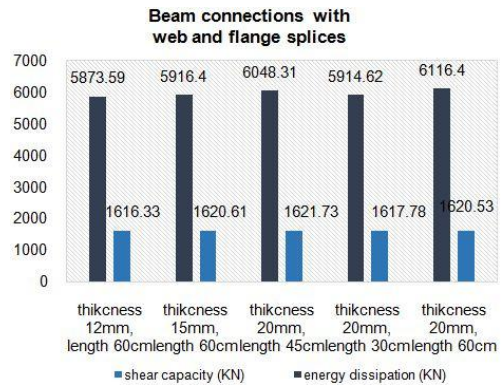Fig. 15 Rigid connection with upper and lower beam plates with plates of various lengths and thicknesses



Fig. 16 Beam connection with web and flange splices of various lengths and thicknesses

fairly bigger than the area encompassed by the hysteresis curve of Con.5. Then, as a practical application, for design of BRB steel structures under cyclic loads such as earthquake, use of Con. 6 is recommended by this study.

Considering that energy absorption and cyclic behavior of BRB frames are functions of the type of beam-column connections, it seems that the current design provisions should have paid more attention to calculation of BRB frames seismic response modification factors ($R$ factor) based on beam-column connection types. The fact that in the existing design codes the impact of connection types is not accurately reflected in the calculation of the R factor of BRB frames has also been expressed by other researchers such as Wigle and Fahnestock (2010).

### 3.3 Study of effective parameters

In this section, the effects of such factors as the length and thickness of simple connection angles and those of rigid connection plates on the behavior of the BRB frames under cyclic loads is investigated.

In Fig. 14 shear capacities and energy dissipation capabilities for three types of simple connections with web angles with various lengths and thicknesses are compared. Results show that the change in the length and thickness of the angle in simple connections has little effect (less than 4%) on the overall frame behavior. Moreover, results of cases incorporating rigid connections with upper-lower beam plates and beam splices with plates of different lengths and thicknesses are presented in Figs. 15 and 16. Results show that the variation of lengths and thicknesses of the plates in rigid connections has a slight effect (not more than 4%) on the overall frame behavior. Therefore, the change in connection factors does not play a significant role in the BRB frame behavior.

### 3.4 Stress evaluation

In this section, stress distribution in different parts of the frames and connections are evaluated. The contour plot of Von Mises stress for rigid connections with beam web and flange splices at story drift of 2% is depicted in Fig. 17. Furthermore, the details of stress contours corresponding to this rigid connection is shown in Fig. 18. These figures show that the maximum stress has occurred in the beam-column connection region. It should be noted that in accordance with Table 1, the type of steel used for the components of the frame is different, and hence the strength of the steel used in the beams and columns is more than that of the core plate. For all frames with different beam-column connections, yielding occurred in the core plate before it did
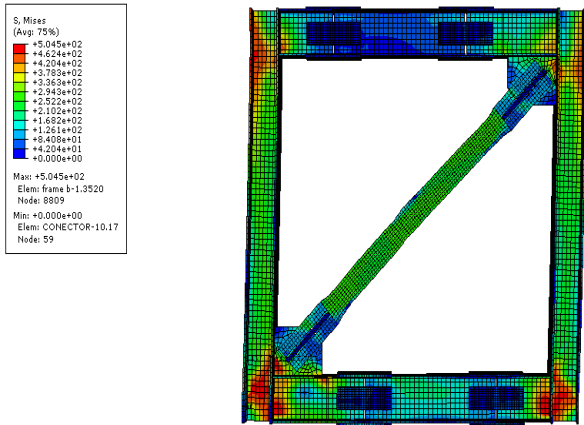
Fig. 17 Von Mises stress contours of the beam connection with web and flange splices
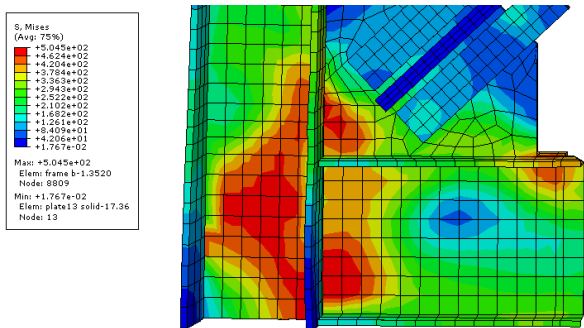


Fig. 18 Von Mises stress contours of the beam connection with web and flange splices

in other frame members. Strength deterioration for all cases occurred in a story drift angle of approximately 2% and all core plates yielded in this story drift as demonstrated in Table 4.

Table 4 Numerical finite element analyses results for different connections at the strength deterioration points

| Con. No. | Connection type | Story drift (%) | Core yield stress (MPa) | Core ultimate stress (MPa) |
|---|---|---|---|---|
| Con. 1 | With web and seat angles | 2.04 | 240 | 289.1 |
| Con. 2 | With seat angle | 2.01 | 240 | 293.9 |
| Con. 3 | With web angle | 2.04 | 240 | 296.7 |
| Con. 4 | With upper-lower beam plates | 2.04 | 240 | 298.8 |
| Con. 5 | Welded rigid connection | 2.02 | 240 | 296.3 |
| Con. 6 | With beam web and flange splices | 2.03 | 240 | 294.1 |

One of the underlying requirements of BRBs is that overall buckling does not occur until sufficient deformation is attained so that the required ductility is proven to have been provided. This required behavior becomes important as the strength and rigidity of the restraining member are reduced. When the rigidity of the encasing is large enough, the total contact forces acting on the upper and lower encasing walls are approximately balanced with each other and the overall buckling will not occur (Hoveidae and Rafezy 2012). As was explained, in order to decrease the computational effort, by introducing proper boundary conditions the encasing was accounted for only indirectly in the FE model. This is equivalent to assuming the encasing rigidity to be high enough to cause the stresses in the core to reach the ultimate level, as is presented in Table 4.

The comparison of the Von Mises stress contour plots for different rigid and simple connections shows that, in contrast to simple connections where stress concentration occurred in the gusset plate nearby its connection to the beam and column stress, for rigid connections concentration occurred in the beam-column connection region. Most notably, for simple connections the highest stress concentrations were in critical regions, e.g., at gusset-element interfaces due to opening and closing of the connection region. Thus, for a simple connection, when the gusset plate is thinner, Von Mises stresses increase. The research results show that the stresses at the free edges of the gusset plates are controlled due to the opening and closing of the joint. So, in these cases larger (or thicker) gusset plates can result in reduction of the stress. For rigid connection frames, thinner gusset plates also lead to larger stresses whose increase is not very effective since the maximum stress at these frames occurs at beam-column connection regions. In other words, in simple connections the dimensions of the gusset plate considerably control the behavior; however, this is not the case in rigid connections. The Von Mises stress contour of the frames with rigid connections shows that sudden strength deteriorations occur when lower beam-column connections (location wherein cyclic lateral load prototypes were imposed) at the joint edge of the beam-column connections have lost their resistance or when plastic hinges are formed in the column panel zone. It is predicted that when the connecting elements have closely proportioned stiffnesses, stress concentrations are less likely to occur since the demand will be more equally distributed between the two elements. As a practical result, in these cases it is suggested to use reinforcement plates in the column panel zone to improve this undesirable performance and increase the shear capacity of the BRB frame.

## 4. Conclusions

The results of this study introduce the effects of beam-column connections on the behavior of BRB frames. All cases were subjected to cyclically increasing drifts. At first, the results of the finite element analysis were verified by experimental results and then the effects of different parameters were investigated. From this study the following conclusions can be obtained:

- The obtained finite element hysteresis curve properly conformed to the test cyclic responses and showed that the FE model can appropriately simulate the behavior of various BRB frames.
- All of the frames manifested excellent hysteretic behaviors and energy dissipation capabilities.
- Results showed that the beam-column connection type had little effect on the maximum story drift in various BRB frames as all BRB frames reached the story drift angle of approximately 2%.
- There was a minor difference in the BRB frame shear capacities for various beam-column connections. The difference between those for frames involving rigid, semi-rigid and simple connections is less than 10%.
- The type of beam-column connection has a significant impact on the dissipated energy and cyclic behavior of BRB frames. The energy dissipation of the frame with rigid connections with beam web and flange splices (Con.6) was 25% greater than that of the frame with continuous beams with welded rigid connections (Con.5).
- It appears that the current design provisions should pay more attention to calculation of the BRB frame seismic response modification factors (R factor) based on the beam-column connection types.
- The change in the lengths and thicknesses of the angles in simple connections and the change in lengths and thicknesses of the plates in rigid connections have little effect (less than 4%) on the overall frame behavior.
- The calculated stress distributions in the core plates show that all core plates are yielded when strength deteriorations occur.
- The comparison of Von Mises stress contour plots for different rigid and simple connections shows that the stress concentration occurred in the beam-column connection region for rigid connections in contrast to simple connections where stress concentration occurred in the gusset plate.
- For simple connections, the highest stress concentrations were at gusset-element interfaces. So, in these cases larger (or thicker) gusset plates can reduce the stress demands.
- For rigid connection frames, the maximum demands (stress concentrations) occurred at the beam-column connection regions. Therefore, to improve the performance and increase the shear capacity of BRB frames, use of reinforcement plates in the column panel zones is suggested.
- Finally, rigid beam-column connections with web and flange splices lead to great energy absorption and the frame's hysteresis performance will be better, compared to when other studied rigid, semi-rigid or simple welded connections are used.

## References

Abaqus (2012), Abaqus 6.12, Analysis and Theory Manual, Simulia, Dassault Systems.

Aiken, I., Mahin, S.A. and Uriz, P. (2002), "Large-scale testing of buckling-restrained braced frames", *Proceedings of Japan Passive Control Symposium*, Japan.

AISC (2005), Seismic Provisions for Structural Steel Buildings, American Institute of Steel Construction, Chicago, IL, USA.

ANSI/AISC 360-10 (2010), Specification for structural steel buildings, AISC Committee on Specifications.

ASCE (2005), Minimum Design Loads for Buildings and other Structures; American Society of Civil Engineers, ASCE/SEI 7-05.

Assaleh, K., AlHamaydeh, M. and Choudhary, I. (2015), "Modeling nonlinear behavior of Buckling-Restrained Braces via different artificial intelligence methods", *Appl. Soft Comput.*, **37**, 923-938.

Christopulos, A.S. (2005), "Improved seismic performance of buckling restrained braced frames", Ph.D. Thesis; University of Washington, Seattle, WA, USA.

Chou, C.-C. and Chen, S.-Y. (2010), "Subassemblage tests and finite element analyses of sandwiched buckling-restrained braces", *Eng. Struct.*, **32**(8), 2108-2121.

Chou, C.-C. and Chung, P.-T. (2014), "Development of cross-anchored dual-core self-centering braces for seismic resistance", *Constr. Steel Res.*, **101**, 19-32.

Chou, C-C., Chen, Y.-C., Pham, D.-H. and Truong, V.-M. (2014), "Steel braced frames with dual-core SCBs and sandwiched BRBs: Mechanics, modeling and seismic demands", *Eng. Struct.*, **72**, 26-40.

Clark, P., Aiken, I., Kasai, K., Ko, E. and Kimura, I. (1999), "Design procedures for buildings incorporating hysteretic damping devices", *Proceedings of the 68th Annual Convention*, Structural Engineers Association of California, Santa Barbara, CA, USA, September-October.

Eurocode 3-Part 1-8 (2005), Design of steel structures; Part 1-8: Design of Joints, European Committee for Standardization.

Fahnestock, L.A., Ricles, J.M. and Sause, R. (2007), "Experimental evaluation of a large-scale buckling-restrained braced frame", *Struct. Eng.*, **133**(9), 1205-1214.

Fanaie, N. and Afsar Dizaj, E. (2014), "Response modification factor of the frames braced with reduced yielding segment BRB", *Struct. Eng. Mech., Int. J.*, **50**(1), 1-17.

Faridmehr, I., Tahir, M.M. and Lahmer, T. (2016), "Classification system for semi-rigid beam-to-column connections", *Latin Am. J. Solids Struct.*, **13**(11), 2152-2175.

Flogeras, A.K. and Papagiannopoulos, G.A. (2017), "On the seismic response of steel buckling-restrained braced structures including soil-structure interaction", *Earthq. Struct.*, **12**(4), 469-478.

Ghowsi, A.F. and Sahoo, D.R. (2015), "Fragility assessment of buckling-restrained braced frames under near-field earthquakes", *Steel Compos. Struct., Int. J.*, **19**(1), 173-190.

Hadianfard, M.A. and Khakzad, A.R. (2016), "Inelastic buckling and post-buckling behavior of gusset plate connections", *Steel Compos. Struct., Int. J.*, **22**(2), 411-427.

Hadianfard, M.A. and Rahnema, H. (2010), "Effects of RHS face deformation on the rigidity of beam-column connection", *Steel Compos. Struct., Int. J.*, **10**(6), 491-502.

Hadianfard, M.A., Khakzad, A.R. and Vaghefi, M. (2015), "Analysis of the effect of stiffener on the buckling capacity and non-elastic behavior of bracing gusset plates", *Scientia Iranica*, **22**(4), 1449-1456.

Hadianfard, M.A., Hashemi, A. and Gholami, M. (2017), "Study on the effects of various mid-connections of x-brace on frame behavior", *Earthq. Struct., Int. J.*, **12**(4), 449-455.

Hoveidae, N. and Rafezy, B. (2012), "Overall buckling behavior of all-steel buckling restrained braces", *Constr. Steel Res.*, **79**, 151-158.

Kim, S.H. and Choi, S.M. (2015), "Structural behavior of inverted

V-braced frames reinforced with non-welded buckling restrained braces", *Steel Compos. Struct.*, *Int. J.*, **19**(6), 1581-1598.

Lin, P.-C., Tsai, K.-C., Wang, K.-J., Yu, Y.-J., Wei, C.-Y., Wu, A.-C., Tsai, C.-Y., Lin, C.-H., Chen, J.-C., Schellenberg, A.H., Mahin, S.A. and Roeder, C.W. (2012), "Seismic design and hybrid tests of a full-scale three-story buckling-restrained braced frame using welded end connections and thin profile", *Earthq. Eng. Struct. Dyn.*, **41**(5), 1001-1020.

Palmer, K.D., Christopulos, A.S., Lehman, D.E. and Roeder, C.W. (2014), "Experimental evaluation of cyclically loaded, large-scale, planar and 3-d buckling restrained braced frames", *Constr. Steel Res.*, **101**, 415-425.

Prinz, G.S. (2007), "Effect of beam splicing on seismic response of buckling restrained braced frames", M.Sc. Thesis; Brigham Young University, Provo, UT, USA.

Razavi-Tabatabaei, S.A., Mirghadri, S.R. and Hosseini, A. (2014), "Experimental and numerical developing of reduced length buckling-restrained brace", *Eng. Struct.*, **77**, 143-160.

Talebi, E., Tahir, M., Zahmatkesh, F. and Kueh, A. (2015), "A numerical analysis on the performance of buckling restrained braces at fire-study of the gap filler effect", *Steel Compos. Struct.*, *Int. J.*, **19**(3), 661-678.

Tremblay, R., Poncet, L., Bolduc, P., Neville, R. and Devall, R. (2004), "Testing and design of buckling restrained braces for Canadian application", *Proceedings of the 13th World Conference on Earthquake Engineering*, Vancouver, BC, Canada, August.

Watanabe, A., Hitomi, Y., Saeki, E., Wada, A. and Fujimoto, M. (1998), "Properties of brace encased in buckling restraining concrete and steel tube", *Proceedings of the 9th World Conference on Earthquake Engineering*, Tokyo-Kyoto, Japan, August, Vol. IV, pp. 719-724.

Wigle, V.R. and Fahnestock, L.A. (2010), "Buckling-restrained braced frame connection performance", *Constr. Steel Res.*, **66**(1), 65-74.

*CC*